JURNAL PENDIDIKAN TEKNOLOGI KEJURUAN

Vol. 5, No. 2 May 2022 **P-ISSN: 2621-3273**
E-ISSN: 2621-1548

Anticorrosive epoxy coatings enhanced with rice husk derived-graphene

Dinda Putri Amalia* **and Rini Riastuti**

Department of Metallurgical and Materials Engineering, Universitas Indonesia, **INDONESIA**

*Corresponding author: dinda.putri01@ui.ac.id

https://doi.org/10.24036/jptk.v5i2.26823

Abstract—Coatings are the most common corrosion control practice. Therefore, it is very important to discover the most cost-effective and environmentally-friendly coating materials for sustainability. When dispersed in epoxy resin, graphene has barrier properties that improve the anticorrosive performance of the metal significantly. Graphene can be synthesized from agricultural waste. Herein, graphene derived from rice husk and epoxy resin was developed with solution mixing to prepare graphene-epoxy coating composites with enhanced anti-corrosive properties. X-ray diffraction, UV-vis spectroscopy, and scanning electron microscopy were used to characterize the synthesized graphenes. The anticorrosive properties of the coatings were characterized by potentiodynamic polarization and electrochemical impedance spectroscopy, which resulted in the corrosion resistance of synthesized graphene and commercial reduced graphene oxide being better than commercial graphene. The impedance and corrosion rate values of synthesized graphene are 1.77 x 10^5 Ω and 0.00011 mm/year.

Keyword: *rice husk, graphene, epoxy resin, corrosion*

I. INTRODUCTION

Corrosion control practices are common and proven to reduce total corrosion costs by 15-35% (NACE International, 2016). The most popular, simple, and adjustable for various components of corrosion control practices is coating. Among the coating classifications, organic or polymeric coatings have a wider range of applications, from automotive to construction. However, the disadvantages of this traditional polymer coating are that it is easy to form defects and has a short service life (Kausar, 2019).

Therefore, one way to work around this is by adding a dispersed filler in the polymer resin, which acts as a composite matrix for the organic coating material, and the promising filler material is graphene. Graphene is categorized as two-dimensional (2D) consisting of sp2 bonds of carbon atoms arranged in a hexagonal lattice (Zhang, Yu, Yang, Cui, & Li, 2021). When graphene is dispersed in a resin polymer, it can act as a barrier and form a diffusion pathway to increase anti-corrosion properties (Mahato & Cho, 2016). One of the most common methods to synthesize graphene with chemical exfoliation methods is Hummer modified. This method use of strong acids can introduce atomic defects into the graphene sheets and problems with toxic chemical waste. Therefore, some research reported the latest development of synthesis by utilizing agricultural waste, which is cost-effective, scalable production, and environmentally friendly (Ismail, et al., 2019).

The graphene was synthesized from agricultural waste by activating carbon with a catalyst, washing with deionized water, and sonication (Muramatsu, et al., 2014) (Singh, Bahadur, & Pal, 2017). In this study, epoxy was used as a polymer matrix for the coating base due to its greater hardness and higher adhesion (Kausar, 2019). Meanwhile, graphene was synthesized from rice husk waste due to its high availability and iron (III) chloride was used as a chemical agent due to its toxicity and activity in graphitization to form a less porous (Kamal, Othman, & Jabarullah, 2020).

II. METHODS

A. Preparation of synthesized graphene

Firstly, the rice husk was rinsed with distilled water and then dried. The rice husk was carbonized inside a muffle furnace at 400 °C for 2 h, and the

result was called rice husk ash (RHA). It was then ground and sieved with # 325. The oversize RHA was called a sacrificial RHA. Afterward, the RHA was activated with a ratio of impregnation of 1:5 (RHA: 2 M $FeCl_3$ solution). The mixture was stirred with a magnetic hotplate for 8 h at 45 ℃, then evaporated in a drying oven at 110 ℃ for 48 h. The impregnated RHA was compacted in a ceramic crucible and put into the middle of a larger crucible. The void around the ceramic crucible was completely closed by sufficiently compacting the sacrificial RHA. The function of the sacrificial RHA was to suppress oxidation when the mixture was heated at graphitization temperature.

Then, the impregnated RHA in ceramic crucibles was graphitized inside a muffle furnace for 2 h at 800 °C. Following the chemical activation treatment, the sample was desilicated in 1.5 M NaOH solution with a magnetic hotplate for 1 h at 80°C, and then neutralized and centrifuged using distilled water. After that, the sample was ultrasonically agitated in deionized water for 5 min. Next, the sample was rinsed using a vacuum filter and dried in a drying oven for 24 h at 40 °C to remove moisture. The solid powder was obtained from that process, called synthesized graphene.

B. Preparation of graphene-epoxy coatings

In this study, graphene-epoxy coatings were prepared by solution mixing. Firstly, different contents of synthesized graphene powder (0, 0.25, and 0.5 wt.%) were mixed with 15 mL of thinner epoxy and ultrasonically stirred for 20 min to get a dispersed graphene solution. Then, 60 g of epoxy resin was added to the mixture and stirred at high speed with a magnetic hotplate for 30 min. Afterward, 40 g of polyamide hardener was added to this mixture and stirred slowly to prevent bubbling. The carbon steel (CS grade A36) plate was polished with sandpaper (grit 80, 240, 500, 1000, and 1500) before coating, degreased with distilled water and alcohol, and then dried. The coating was uniformly applied to the surface of the CS plate by a simple dipping method, evaporated at room temperature, and then cured in an oven at 80 °C for 2 h. Epoxy coatings without graphene content (EP), synthesis graphene (0.25 wt.%) (G025), synthesis graphene (0.5 wt.%) (G05), commercial graphene (0.5 wt.%) (GN05), commercial reduced graphene oxide (RGO) (0.5 wt.%) (RG05), and bare CS plate (CS) were prepared using the same method.

C. Characterization

An Empyrean intelligent diffractometer with a 40 kV acceleration voltage and a current of 30 mA was used to perform X-ray diffraction (XRD) analysis. The intensity data were collected in the 5–80° range using a step scan mode with CuK radiation (λ= 1.5406). The optical characterization was carried out at room temperature in colloidal solution form in a UV Quartz cuvette in the wavelength range of 200 to 800 nm with distilled water as a control using a Genesys 10S UV-Vis spectrophotometer. A flat cell with three electrodes was created for the corrosion studies, with a coated steel panel as the working electrode, platinum as the counter electrode, and an Ag/AgCl electrode as a reference electrode. An Autolab PGSTAT302N was used to perform electrochemical impedance spectroscopy (EIS) and potentiodynamic polarization curves. Nova 1.11 software was used to fit the circuit equivalent. The morphology of graphene were determined using scanning electron microscopy (SEM), a Quanta 650 instrument.

III. RESULTS AND DISCUSSION

A. Characteristics of Synthesized Graphene

From Figure 1 (a), it can be seen that synthesized graphene displays some peaks centered at 2 values of 10.65°, 22.9°, and 44.03°, corresponding to the inter-layer spacing of 8.3, 3.88, and 2.05Å, respectively, calculated using the Bragg equation. The obtained d value (8.3Å) at 10.65° is more than double that of pristine graphite (d~ 3.34Å), indicating that the graphitic stack has expanded due to the production of oxidation-generated polar functionalities over the graphene layer (Sharma, Chadha, & Saini, 2017). Meanwhile, the obtained d value (3.88Å) at 22.9° corresponds to aromatic layer reflection in the (002) plane, while a peak is barely visible at 44.03° (d= 2.05Å) relating to aromatic layer reflection in the (100) plane. The better the orientation of the aromatic layer slice, the smaller and higher the (002) peak. The aromatic layer slice is greater when the (100) peak is smaller and higher (Zhang, Yu, Yang, Cui, & Li, 2021). As a result, a few very small graphene microcrystalline formations have been identified.

Figure 1 (b) shows the optical absorption properties of sythesized graphene. The first is a shoulder at 306 nm, which corresponds to an n-π* plasmon peak, which is attributed to the transition of C-O bonds entrenched on the graphene via exfoliation and intercalation. Another distinguishing feature is a π-π* plasmon peak at 228 nm, which is related to an aromatic C-C ring transition (Thema, et al., 2013).

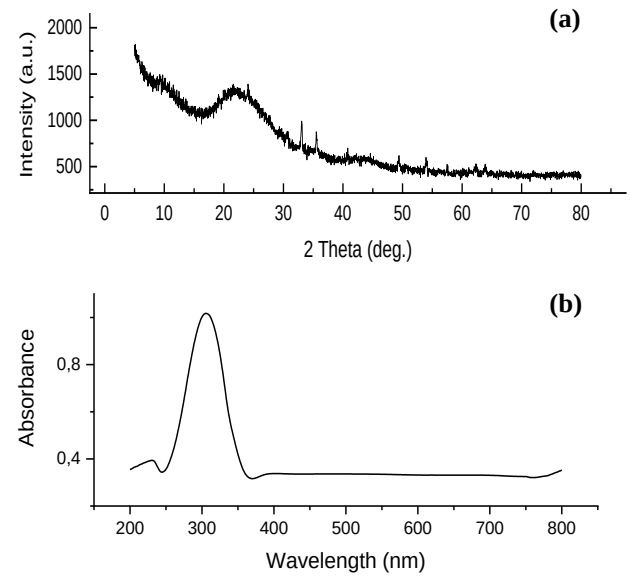

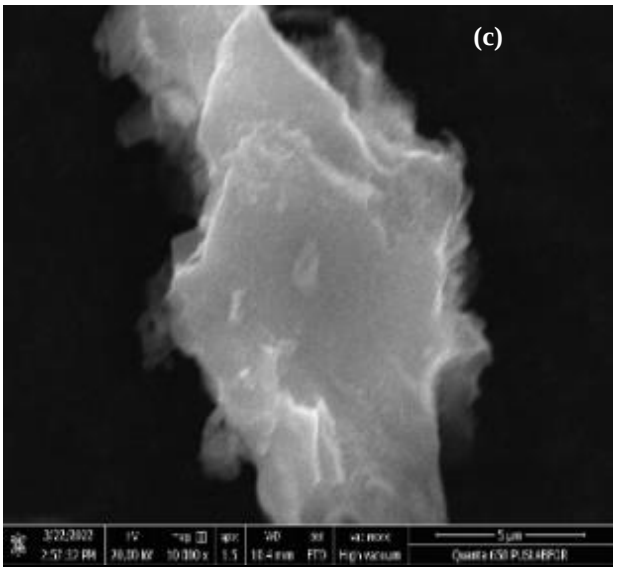

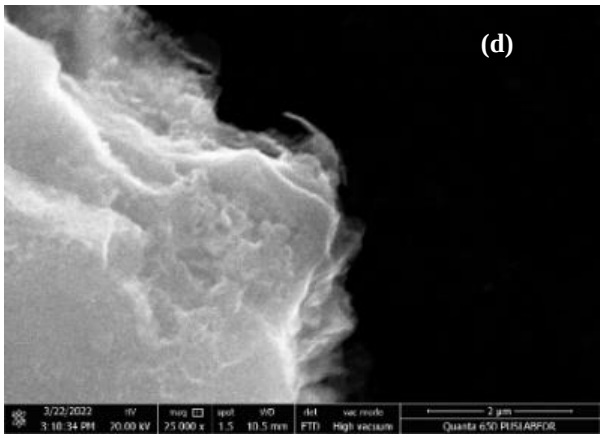

Figure 1. (a) XRD patterns of synthesized graphene powder, (b) UV-Vis spectra of synthesized graphene dispersion, SEM morphology of synthesized graphene (c) 10.000x and (d) 25.000x magnification

Therefore, as determined by the absorbance value, the optical absorption result is dominated by the n-π* plasmon peak near 306 nm which indicates graphene was synthesized. From Figure 1 (c) and (d), it can be seen that synthesized graphene displays some stacked layers due to new C=C double bonds being formed, then weakened electrostatic repulsion between graphene layers, and the absence of active functional groups that increase agglomerates (Wang & Cai, 2020). As shown in Figure 1 (c), in the center of layers are less porous or defective because there was no redox process on hydroxyl groups on benzene ring branches. However, as shown in Figure 1 (d), the edges of the layer are more defective due to the shear force at a high frequency applied when ultrasonication breaks graphene layers into pieces (Yang, Liu, Fan, & Zhang, 2020).

B. Characteristics of Synthesized Graphene-Epoxy Coatings

Figure 2 shows the potentiodynamic polarization curves of various coatings in a 3.5 wt. % NaCl solution. The intersection of the tangent line of the anodic and cathodic polarization curves provides the values of corrosion potential (E_{corr}) and corrosion current density (i_{corr}). The corrosion rate (CR) of the samples were determined using the Equation (1) below:

$$CR = 3.27\, a i_{corr} / nD \quad (1)$$

D denotes the density, *a* denotes the atomic or molecular weight, and *n* denotes the number of equivalents exchanged. Figure 2 (a) shows the potentiodynamic polarization curve of bare CS plate and coatings with different content of graphene, correspondingly, the value of CR was determined to be 1.1 x 10^{-4}, 1.6 x 10^{-3}, 2 x 10^{-3}, and 0.25 mm/year, increasing in the sequence G05 < G025 < EP < CS. It was discovered that epoxy composite coatings with graphene content of 0.5 wt. % have much better corrosion resistance than those with graphene content of 0.25 wt. %. From Figure 2 (a), it can be inferred that increasing the graphene content increases the corrosion resistance due to its longer diffusion pathway (Mahato & Cho, 2016). Therefore, graphene content of 0.5 wt.% parameter was used for the study of epoxy composite coating corrosion resistance with different graphene derivatives.

Figure 2 (b) shows the potentiodynamic polarization curve of different graphene derivatives samples, correspondingly, the value of CR was determined to be 3 x 10^{-5}, 1.1 x 10^{-4}, and 7.1 x 10^{-4} mm/year, increasing in the sequence RG05 < G05 < GN05. Compared with all samples, RG05 and G05

displayed better anti-corrosion performance than GN05 due to the presence of a few graphene oxides that have larger inter-layer spacing (0.75-0.95 nm) than pristine graphene (~0.34 nm) (Thema, et al., 2013). RG05 has better corrosion resistance than G05 because the reduced graphene oxide molecules can cover the active anode sites and suppress the corrosion with pore plugging (Zhang, Yu, Yang, Cui, & Li, 2021). Meanwhile, a few graphene oxides in synthesized graphene require reduction first before covering the anode sites.

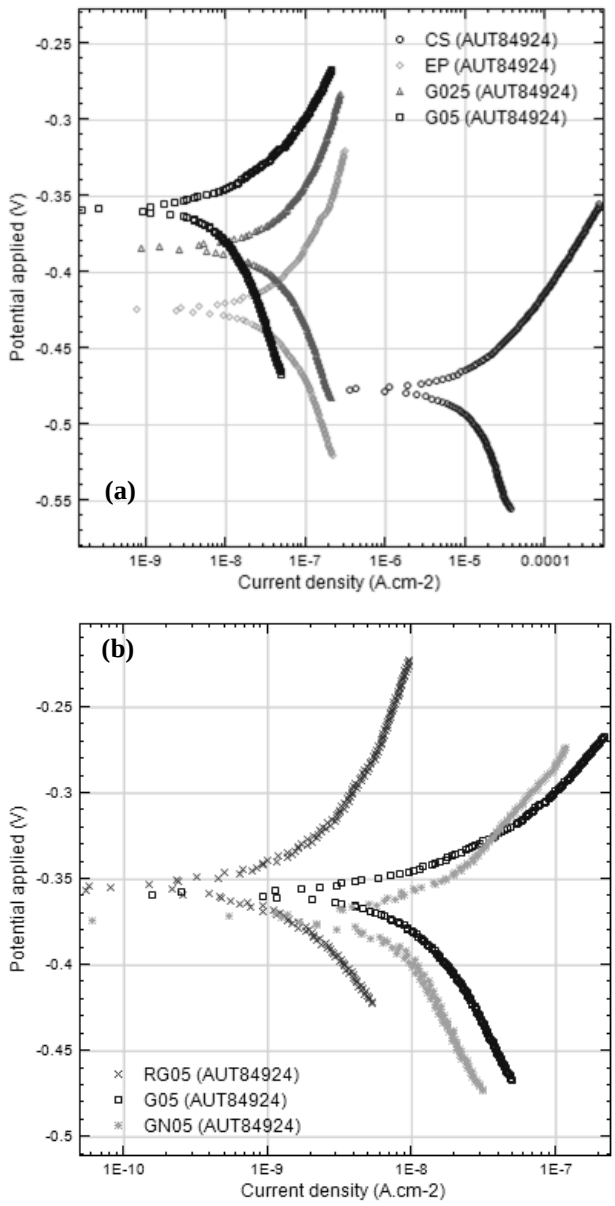

Figure 2. Linear polarization results of Graphene-Epoxy Coatings (a) different graphene content, (b) different graphene derivatives

The EIS results of different graphene derivatives coatings in a 3.5 wt. % NaCl solution can be seen in Figure 3 (a) and (b). The larger the diameter of the capacitive arc, as seen in Nyquist plots in Figure 3 (a), the higher the sample's corrosion resistance. The diameters of the capacitive arc from the Nyquist plot match the order of the Bode phase diagram, indicating that the results are consistent. The value of impedance at a low frequency of 0.01 Hz for different samples was determined to be 1.77 x 10^5, 1.74 x 10^5, and 1.29 x 10^5 Ω, decreasing in the sequence G05 > RG05 > GN05. It can be found that the corrosion resistance of epoxy composite coatings with synthesized graphene and RGO is obviously better than with pristine graphene. The high-frequency area of the Bode phase angle diagram corresponds to the coating's protection, whereas the medium and low-frequency areas correspond to the corrosion response between the corrosive environment and metal (Yang, Zhu, & Hong, 2020). According to the Bode phase diagram in Figure 3 (b), the three samples' ability to withstand corrosive environments was increased first, then reduced in the intermediate to low-frequency area.

The EIS data were analyzed using an equivalent circuit model to simulate electrical characteristics (Yang, Yang, Wang, Chen, & Li, 2019). Figure 3 (c) and (d) show the equivalent circuit model, in which Rs (Ω) is denoted to the solution resistance, the charge transfer resistance of the electrode interface and the coating resistance are represented by Rct and Rc (Ω). Coating capacitance is denoted by the letter Cc (F). CPEdl (F) denotes the electrode/solution interface's constant phase elements (CPE), which simulate the behavior of a double layer. The results of a fitting equivalent circuit model for RG05 and G05 were shown in Figure 3 (c). It can be said that RG05 and G05 have the same equivalent circuit model, which indicates good coating. The corrosion protection mechanism corresponding to Cc indicates stored charge from the result of the reduction process graphene or RGO filler of coatings and Rc indicates the resistance of the porous coating. The charge passes through the pore and then contacts the substrate, and, as a result, an inhomogeneous oxide layer is formed, indicated with CPEdl. Meanwhile, Figure 3 (d) was the result of fitting an equivalent circuit for GN05 that indicated a failed coating. The corrosion mechanism, derived from Rct, indicates the corrosion process due to the charge transfer between electrolyte and substrate.

Based on the fitting results in Table 1, Rc for RG05 and G05 were almost the same at 160 and 168 kΩ, respectively. It shows that the corrosion resistance of RG05 and G05 better than GN05 matches the results of CR values from potentiodynamic polarization curves, Nyquist plots and Bode phase diagrams. The value of Cc from RG05 is better than G05 and GN05 due to the conductivity of RGO better than pristine graphene. According to literature, pristine graphene film and

RGO have 0.22 S.cm^{-1} and 15 S.cm^{-1} (Zhang, Yu, Yang, Cui, & Li, 2021). Meanwhile, the value of Rct in GN05 indicates the resistance when charge is transferred between the interface electrolyte and substrate. The value of Y0 from GN05 is smaller than RG05 and G05 due to the inhomogeneity of the oxide layer that is produced by GN05. These values are supported by the value of N from RG05 near zero, indicate that there is low activity of the double-layer dominant with capacitive activity (Yang, Yang, Wang, Chen, & Li, 2019). The opposite of the value of N from GN05 is more than one, indicating that there is high activity of the double-layer due to charge transfer that results in substrate degradation.

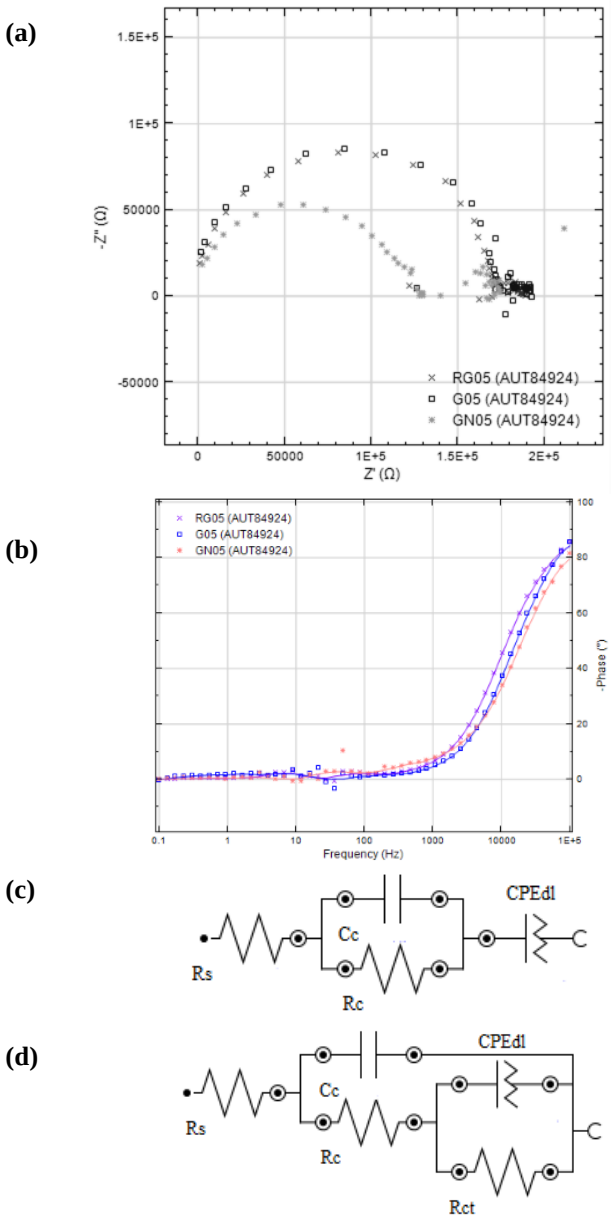

Figure 3. EIS results of (a) Nyquist plots, (b) Bode phase angle diagrams, Equivalent circuit model of Graphene-Epoxy Coatings (c) good and (d) failed coating

Table 1 Fitting results of equivalent circuit model

Sample	Rc [kΩ]	Cc [pF]	Rct [kΩ]	CPEdl [pF]	
				Y0 [μMho]	N
RG05	160	97.3	-	22.4	0.0749
G05	168	66.3	-	31.8	0.137
GN05	35.5	91.1	174	2.88 x 10^{-3}	1.09

IV. CONCLUSION

Synthesized graphene from rice husk as raw material with the method in this study is possible to be produced cost-effectively and environmentally friendly. The synthesized graphene in this study has characteristics that are more similar to RGO than pristine graphene due to the oxidation process when heat the RHA may not be fully suppressed by sacrificial RHA, resulting in the C-O bonds in the graphitic structure. However, the C-O bonds in the synthesized graphene have the same C-O bonds as graphene oxide and can improve the anticorrosive properties due to the higher inter-layer spacing microcrystalline graphite. Based on electrochemical measurements by linear polarization and EIS, the corrosion resistance of synthesized graphene and RGO is better than pristine graphene because of the ability of molecule-reduced graphene oxide to cover the anode sites that create capacitive electrical characteristics. Therefore, epoxy coating enhanced with graphene derivated from rice husk can be an alternative for anticorrosive coatings.

REFERENCES

Ismail, M., Yusof, N., Yusop, M., Ismail, A., Jafaar, J., Aziz, F., & Karim, Z. (2019). Synthesis and characterization of graphene derived from rice husks. *Malaysian Journal of Fundamental and Applied Sciences, 15*(4), 516-521.

Kamal, A. S., Othman, R., & Jabarullah, N. H. (2020). Preparation and synthesis of synthetic graphite from biomass waste: A review. *Systematic Reviews in Pharmacy, 11*(2), 881-894.

Kausar, A. (2019). Corrosion prevention prospects of polymeric nanocomposites: A review. *Journal of Plastic Film & Sheeting, 35(2)*, 181-202.

Mahato, N., & Cho, M. H. (2016). Graphene integrated polyaniline nanostructured composite coating for protecting steels from corrosion: Synthesis, characterization, and protection mechanism of the coating

material in acidic environment. *Construction and Building Materials, 115*, 618-633.

Muramatsu, H., Kim, Y., Yang, K., Cruz-Silva, R., Toda, I., Yamada, T., . . . Saitoh, H. (2014). Rice husk-derived graphene with nano-sized domains and clean edges. *Small, 10*, 2766-2770.

NACE International. (2016). International Measures of Prevention, Application, and Economics of Corrosion Technologies Study. *IMPACT*.

Sharma, R., Chadha, N., & Saini, P. (2017). Determination of defect density, crystallite size and number of graphene layers in graphene analogues using X-ray diffraction and Raman spectrocopy. *Indian Journal of Pure & Applied Physics, 55*, 625-629.

Singh, P., Bahadur, J., & Pal, K. (2017). Onestep one chemical synthesis process of graphene from rice husk for energy storage applications. *Scientific Research Publishing, 6*, 61-71.

Thema, F., Moloto, M., Dikio, E., Nyawinge, N., Kotsedi, L., Maaza, M., & Khenfouch, M. (2013). Synthesis and characterization of graphene thin films by chemical reduction of exfoliated and intercalated graphite oxide. *Journal of Chemistry*(150536).

Wang, P., & Cai, D. (2020). Preparation of graphene-modified anticorrosion coating study on its corrosion resistance mechanism. *International Journal of Photoenergy*(8846644).

Yang, M., Liu, Y., Fan, T., & Zhang, D. (2020). Metal-graphene interfaces in epitaxial and bulk systems: A review. *Progress in Materials Science, 110*, 100652.

Yang, N., Yang, T., Wang, W., Chen, H., & Li, W. (2019). Polydopamine modified polyaniline-graphene oxide composite for enhancement of corrosion resistance. *Journal of Hazardous Materials, 377*, 142-151.

Yang, S., Zhu, S., & Hong, R. (2020). Graphene oxide/polyaniline nanocomposites used in anticorrosive coatings for environmental protection. *Coatings, 10*(1215).

Zhang, R., Yu, X., Yang, Q., Cui, G., & Li, Z. (2021). The role of graphene in anti-corrosion coatings: A review. *Construction and Building Materials, 294*, 123613.